# From the 1D Schrödinger Infinite Well to Dirac-Weyl Graphene Flakes

Maurício Fitz de Castro Martins Quintela
*Supervisor*: Prof. Dr. João M. B. Lopes dos Santos[1]

[1]Departamento de Física e Astronomia,
Universidade do Porto

December 16, 2019

- The initial objective of this thesis was to study the spectrum of finite regions of twisted bilayer graphene (TBLG).
- In TBLG, a periodic structure emerges for commensurate angles, with the period growing as $\frac{1}{\sin\theta/2}$.
- According to the literature [Tarnopolsky (2019)], the physics of this material is mainly defined by the regions of AA-stacking.

- The initial objective of this thesis was to study the spectrum of finite regions of twisted bilayer graphene (TBLG).
- In TBLG, a periodic structure emerges for commensurate angles, with the period growing as $\frac{1}{\sin\theta/2}$.
- According to the literature [Tarnopolsky (2019)], the physics of this material is mainly defined by the regions of AA-stacking.

- The initial objective of this thesis was to study the spectrum of finite regions of twisted bilayer graphene (TBLG).
- In TBLG, a periodic structure emerges for commensurate angles, with the period growing as $\frac{1}{\sin\theta/2}$.
- According to the literature [Tarnopolsky (2019)], the physics of this material is mainly defined by the regions of AA-stacking.

- The magic angles occur when a specific eigenvalue appears in these regions.
- These regions are hexagons whose boundaries that are approximately zigzag in one of the layers.
- This creates the necessity of finding a method to solve partial differential equations in general polygonal enclosures.

- The magic angles occur when a specific eigenvalue appears in these regions.
- These regions are hexagons whose boundaries that are approximately zigzag in one of the layers.
- This creates the necessity of finding a method to solve partial differential equations in general polygonal enclosures.

- The magic angles occur when a specific eigenvalue appears in these regions.
- These regions are hexagons whose boundaries that are approximately zigzag in one of the layers.
- This creates the necessity of finding a method to solve partial differential equations in general polygonal enclosures.

## Motivation – TBLG

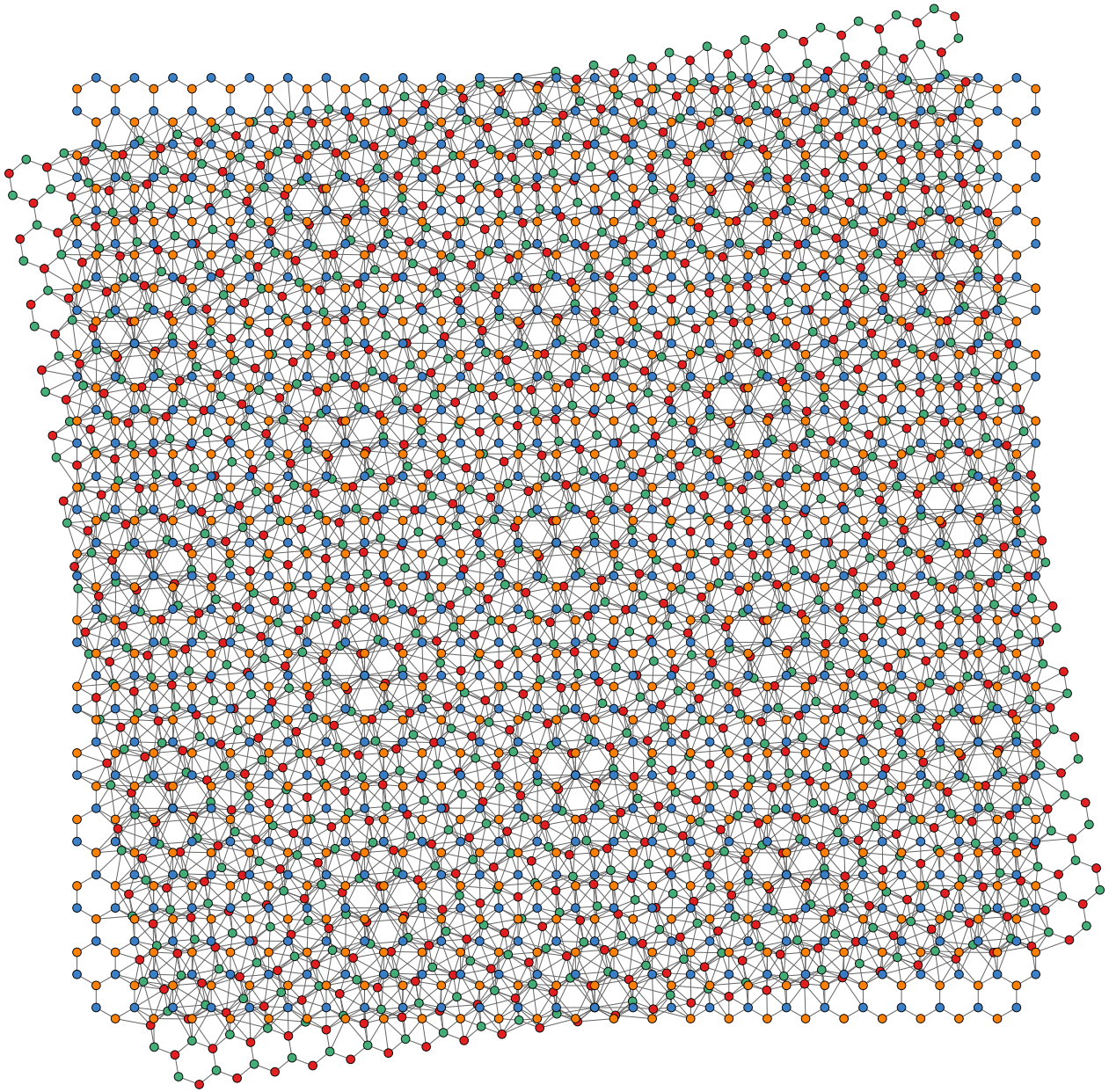

# Separation of Variables

To solve Schrödinger Equation, one usually assumes separation of variables.

$$-\frac{\hbar^2}{2m}\nabla^2\Psi = E\Psi$$

$$\Psi(x,y) = f(x)\,g(y)$$

Applying this to the square infinite potential well, the solution is simply

$$\Psi_{k_x,k_y}(x,y) = \sin(k_x x)\sin(k_y y)$$

The allowed energy eigenvalues are

$$E_{n_x,n_y} = \frac{\hbar^2}{2m}\left(\frac{\pi}{L}\right)^2\left(n_x^2+n_y^2\right)$$

# Separation of Variables

To solve Schrödinger Equation, one usually assumes separation of variables.

$$-\frac{\hbar^2}{2m}\nabla^2\Psi = E\Psi$$

$$\Psi(x,y) = f(x)\,g(y)$$

Applying this to the square infinite potential well, the solution is simply

$$\Psi_{k_x,k_y}(x,y) = \sin(k_x x)\sin(k_y y)$$

The allowed energy eigenvalues are

$$E_{n_x,n_y} = \frac{\hbar^2}{2m}\left(\frac{\pi}{L}\right)^2\left(n_x^2+n_y^2\right)$$

# 2D Generalization

The polynomial method consists of creating a function that obeys boundary conditions,

$$\psi_0(x,y) = N_0 \prod_{s=1}^{n} \varphi_s(x,y),$$

where the different $\varphi_s$ are the equations of the edges of the polygon:

$$y - mx - b = 0$$

The Hamiltonian matrix will also be the 2D analogous of the previous one

$$H_{ij} = -\frac{\hbar^2}{2m} \iint_A dA \psi_i(x,y) \nabla^2 \psi_j(x,y)$$

# 2D Generalization

The polynomial method consists of creating a function that obeys boundary conditions,

$$\psi_0(x,y) = N_0 \prod_{s=1}^{n} \varphi_s(x,y),$$

where the different $\varphi_s$ are the equations of the edges of the polygon:

$$y - mx - b = 0$$

The Hamiltonian matrix will also be the 2D analogous of the previous one

$$H_{ij} = -\frac{\hbar^2}{2m} \iint_A dA \psi_i(x,y) \nabla^2 \psi_j(x,y)$$

# 2D Generalization

The complete basis is defined by Gram-Schmidt orthogonalization

$$\psi_i(x,y) = N_i\left[f_i(x,y)\,\psi_0(x,y) - \sum_{j=0}^{i-1}\langle f_i(x,y)\,\psi_0(x,y)\,|\psi_j(x,y)\rangle\psi_j(x,y)\right]$$

Where $f_m(x,y)$ is a sorting of the $x^i y^j$-monomials as a list [Liew (1991)]

$$f_m(x,y) = \left\{1, x, y, xy, x^2, y^2, x^2y, xy^2, x^2y^2, x^3, y^3, x^3y, xy^3, (\ldots)\right\}.$$

# 2D Generalization

The complete basis is defined by Gram-Schmidt orthogonalization

$$\psi_i(x,y) = N_i\left[f_i(x,y)\,\psi_0(x,y) - \sum_{j=0}^{i-1}\langle f_i(x,y)\,\psi_0(x,y)\,|\psi_j(x,y)\rangle\psi_j(x,y)\right]$$

Where $f_m(x,y)$ is a sorting of the $x^i y^j$-monomials as a list [Liew (1991)]

$$f_m(x,y) = \left\{1, x, y, xy, x^2, y^2, x^2y, xy^2, x^2y^2, x^3, y^3, x^3y, xy^3, (\ldots)\right\}.$$

# Square Infinite Potential Well

The obtained spectrum converges gradually to the exact results

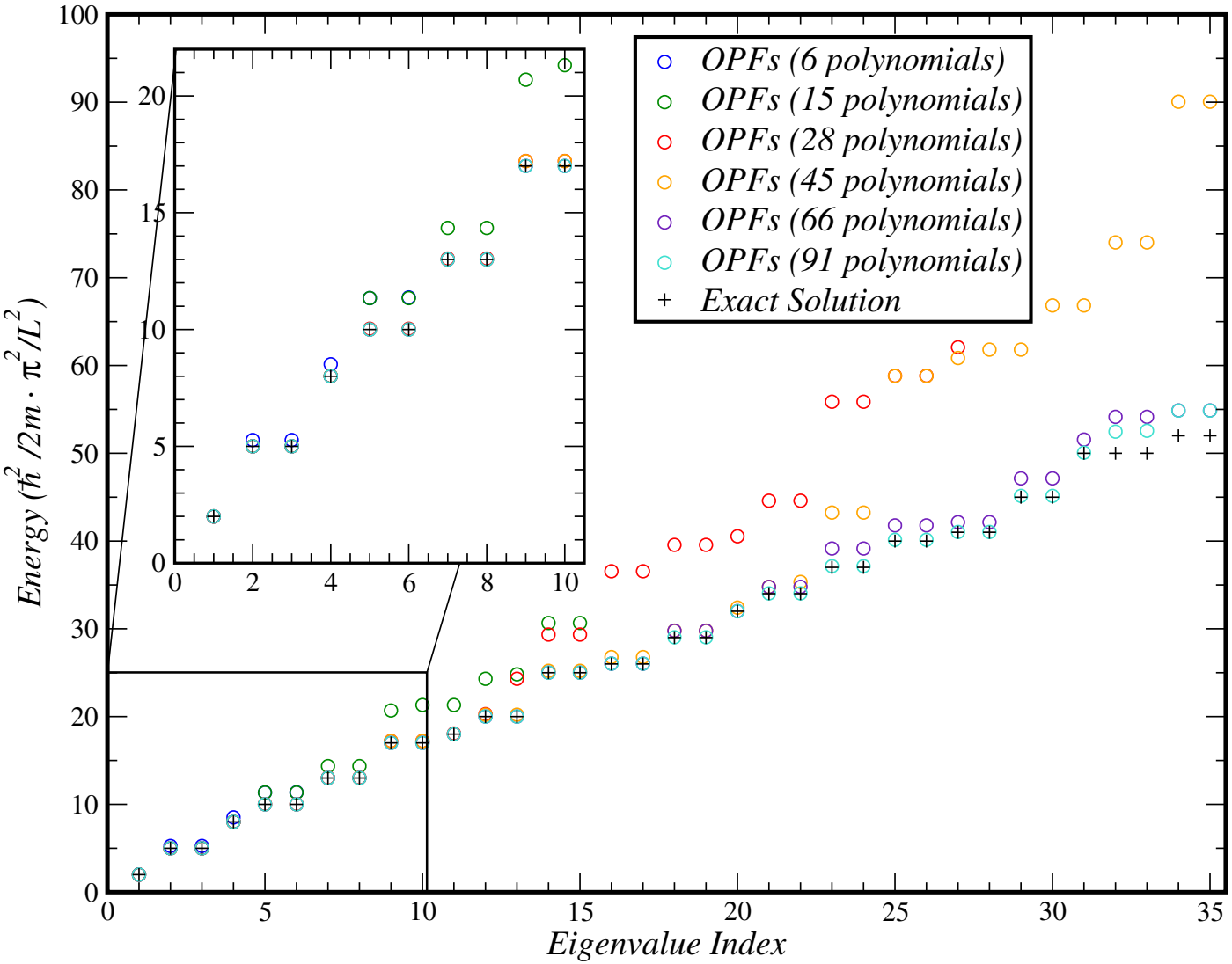

# Square Infinite Potential Well

This $f_m(x, y)$ list can also be built from polynomials that belong to the irreducible representations of the symmetry group of the enclosure in question.

This will accelerate the calculation of the Hamiltonian matrix, but will be require a more involved approach when generating the higher order polynomials.

# Square Infinite Potential Well

This $f_m(x, y)$ list can also be built from polynomials that belong to the irreducible representations of the symmetry group of the enclosure in question.

This will accelerate the calculation of the Hamiltonian matrix, but will be require a more involved approach when generating the higher order polynomials.

# Square Infinite Potential Well

For this specific enclosure, the point-group in question is $C_{4v}$.

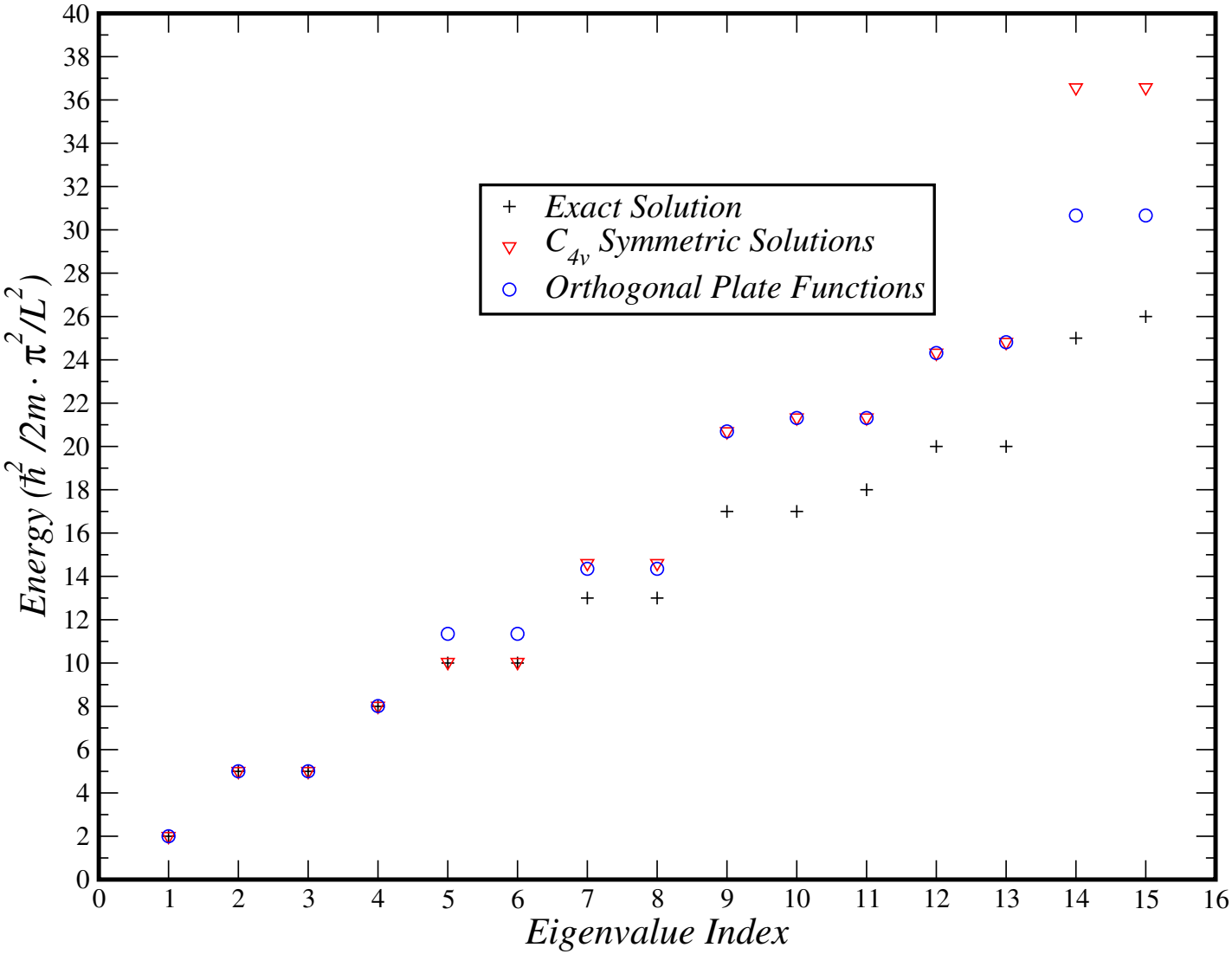

# Hexagonal Infinite Potential Well

The fundamental function will now be a sixth order polynomial, defined in the same way as before

$$\Psi_0(x,y) = N_0 \prod_{s=1}^{6} \varphi_s(x,y)$$

We must define the integration region carefully

$$\iint_A dxdy \rightarrow \int_{-\frac{\sqrt{3}}{2}}^{\frac{\sqrt{3}}{2}} dy \int_{-1+\frac{|y|}{\sqrt{3}}}^{1-\frac{|y|}{\sqrt{3}}} dx$$

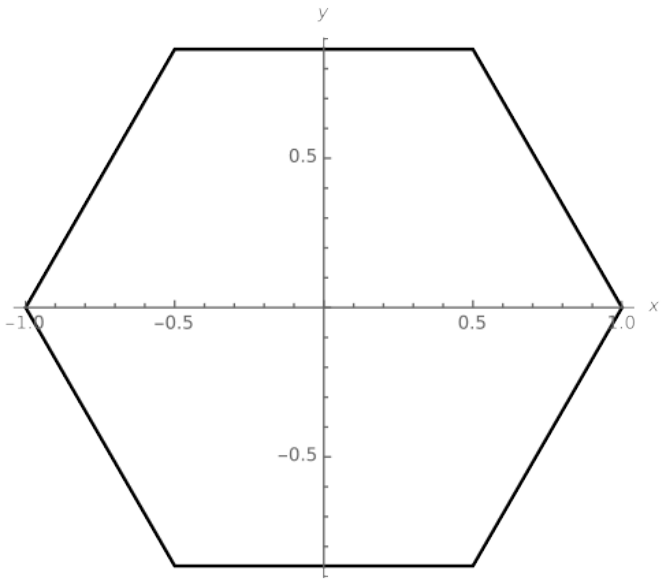

# Hexagonal Infinite Potential Well

The obtained eigenvalues for different basis sizes are as follows

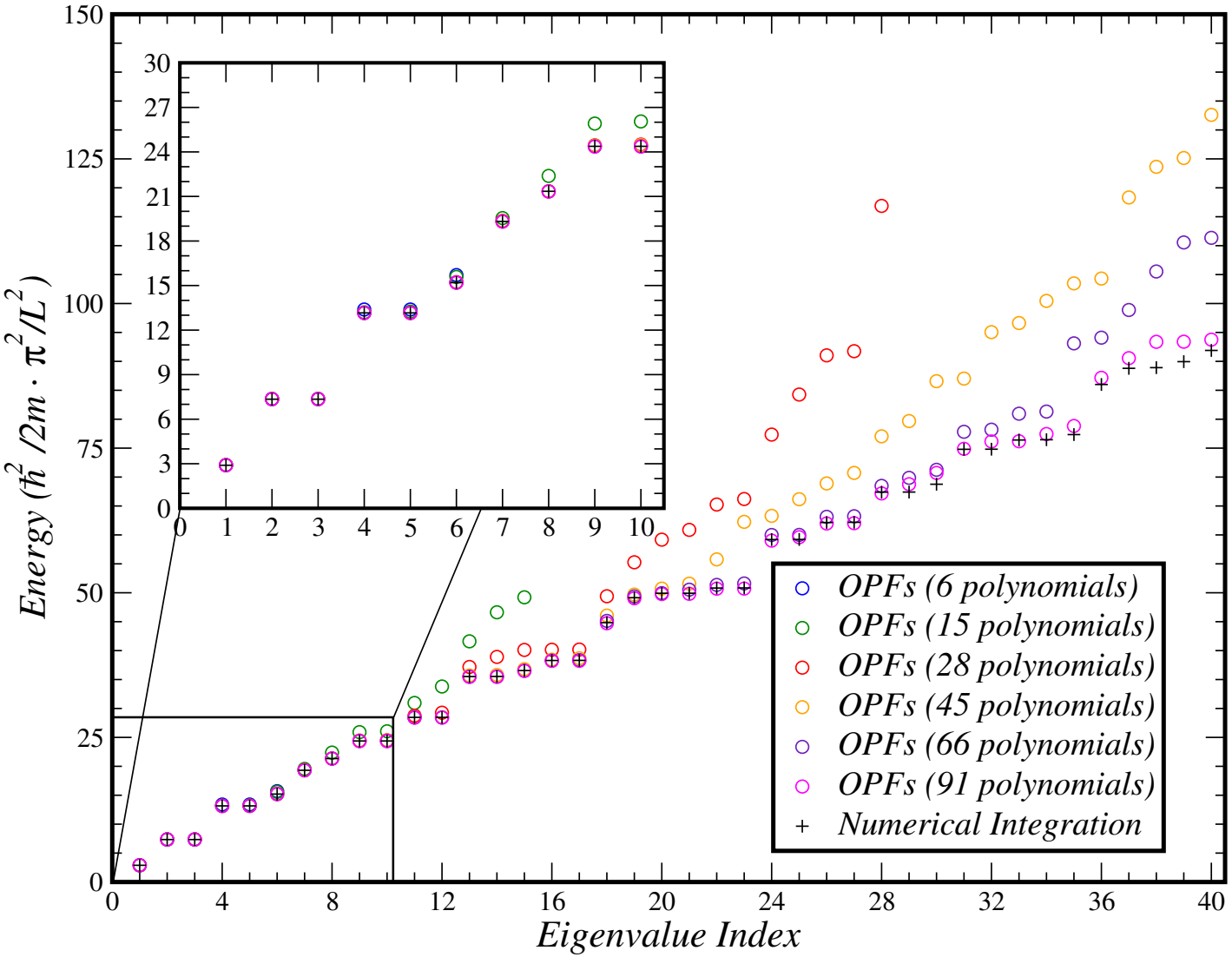

# Exact Solution by Gaddah

Gaddah considers the problem of the triangular graphene dot with $\varphi_A$ terminations on all three edges [Gaddah (2018)].
Considering the system's innate $C_{3v}$ symmetries, the author is able to find analytical expressions for both the eigenfunctions and the eigenvalues of the Dirac Hamiltonian squared.

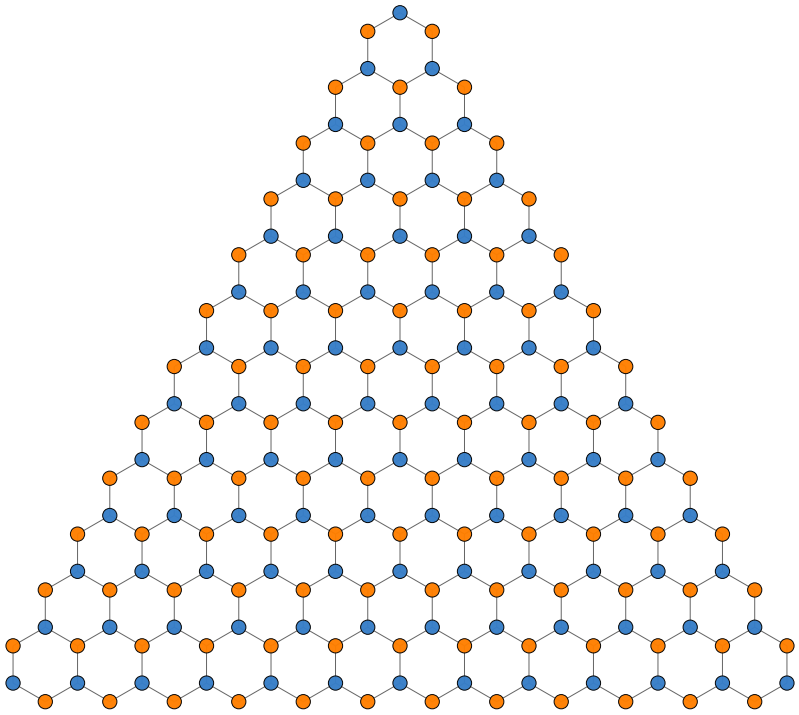

# Exact Solution by Gaddah

If we were to calculate the spectrum of this region with a tight-binding model, there would be many states of exactly zero-energy. How many and why?

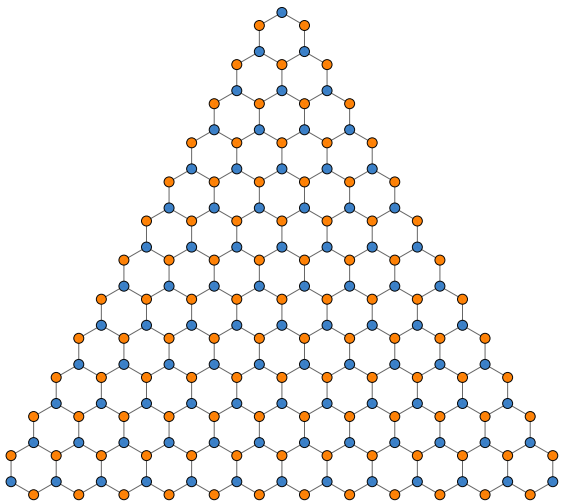

As the Hamiltonian is a linear operator that transforms $\psi_A \leftrightarrow \psi_B$, the dimension of its kernel will be the same as the difference between the dimensions (i.e., number of sites) of each subspace.

# Exact Solution by Gaddah

If we were to calculate the spectrum of this region with a tight-binding model, there would be many states of exactly zero-energy. How many and why?

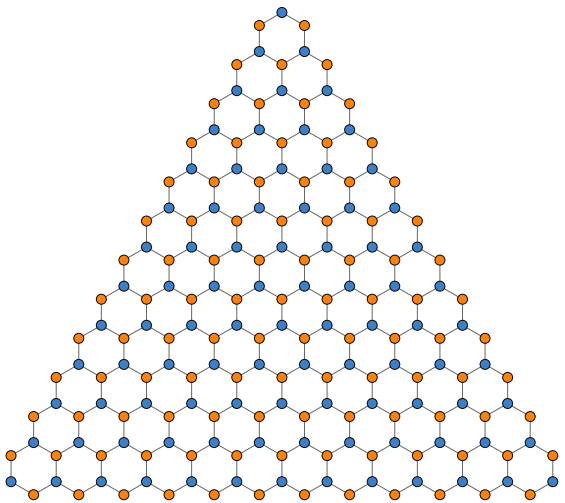

As the Hamiltonian is a linear operator that transforms $\psi_A \leftrightarrow \psi_B$, the dimension of its kernel will be the same as the difference between the dimensions (i.e., number of sites) of each subspace.

# Exact Solution by Gaddah

The Hamiltonian for graphene near the Dirac point $\mathcal{K}$ is given by

$$\mathcal{H}_{\mathcal{K}} = \hbar v_F \vec{\sigma} \cdot \vec{p}$$

where $\sigma$ are the Pauli matrices and $p$ is the momentum operator.

Regarding the boundary conditions, we have that

$$\psi_A = 0$$
$$(\partial_x - i\partial_y)\,\psi_B = 0$$

where $A$, $B$ are the sublattice indices.

# Exact Solution by Gaddah

The Hamiltonian for graphene near the Dirac point $\mathcal{K}$ is given by

$$\mathcal{H}_{\mathcal{K}} = \hbar v_F \vec{\sigma} \cdot \vec{p}$$

where $\sigma$ are the Pauli matrices and $p$ is the momentum operator. Regarding the boundary conditions, we have that

$$\begin{aligned} \psi_A &= 0 \\ (\partial_x - i\partial_y)\,\psi_B &= 0 \end{aligned}$$

where $A$, $B$ are the sublattice indices.

# Exact Solution by Gaddah

The only state of exactly-zero energy one can write that obeys both the boundary conditions and the Dirac equation for this system is

$$\Psi(x,y) = \begin{bmatrix} 0 \\ \frac{2}{\sqrt[4]{3}L} \end{bmatrix}$$

This solution is not present in Gaddah's treatment, and is also not found by our polynomial method, as it is the trivial solution in the sublattice that is being considered ($\psi_A$).

# Exact Solution by Gaddah

The only state of exactly-zero energy one can write that obeys both the boundary conditions and the Dirac equation for this system is

$$\Psi(x,y) = \begin{bmatrix} 0 \\ \frac{2}{\sqrt[4]{3}L} \end{bmatrix}$$

This solution is not present in Gaddah's treatment, and is also not found by our polynomial method, as it is the trivial solution in the sublattice that is being considered $(\psi_A)$.

# Exact Solution by Gaddah

By transforming this problem into a Helmholtz problem, Gaddah obtains the spectrum with a gap of $2\sqrt{3}\frac{4\pi}{3L}\hbar v_F$:

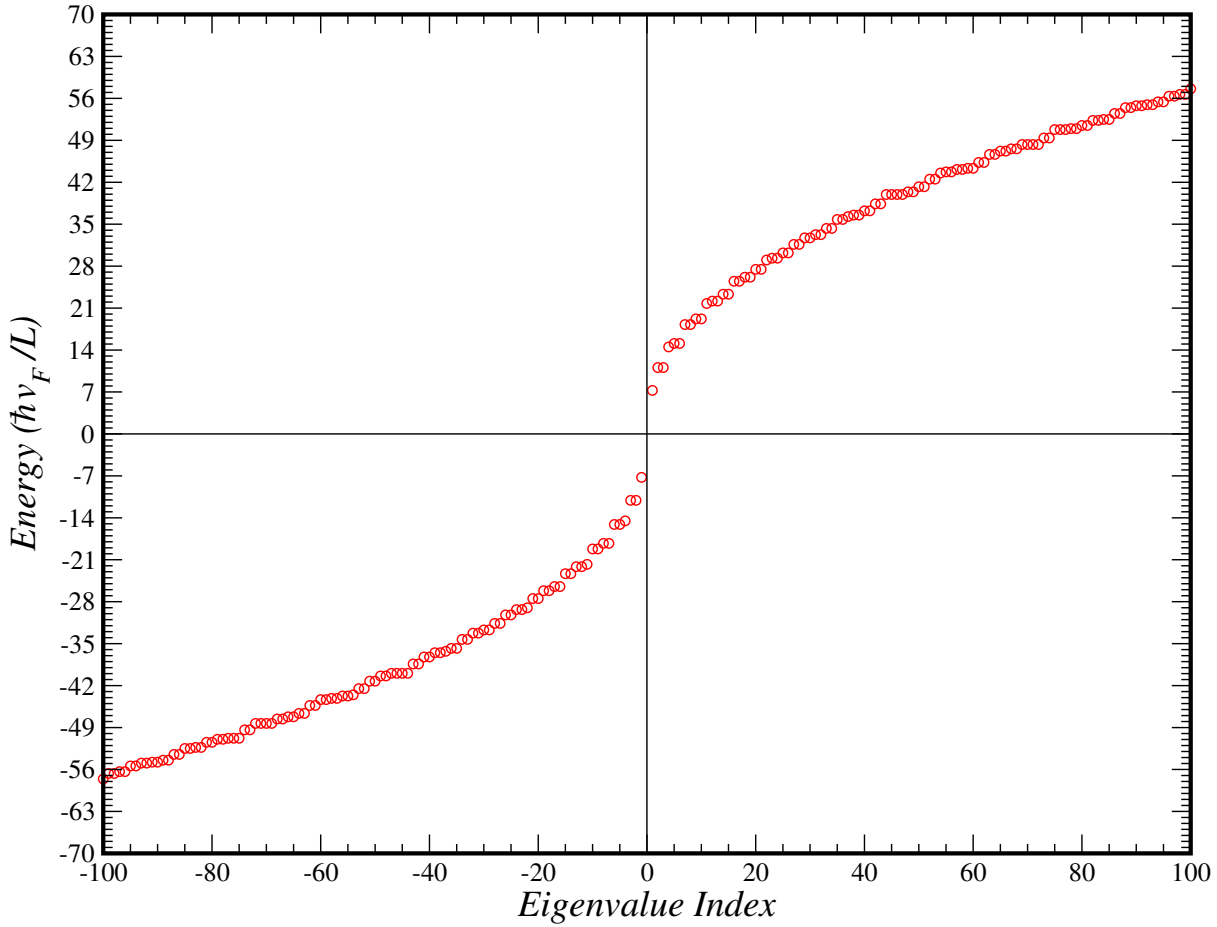

# Polynomial Method

Due to the specific boundary conditions, the polynomial method can be applied in the same way as in the Schrödinger problem.

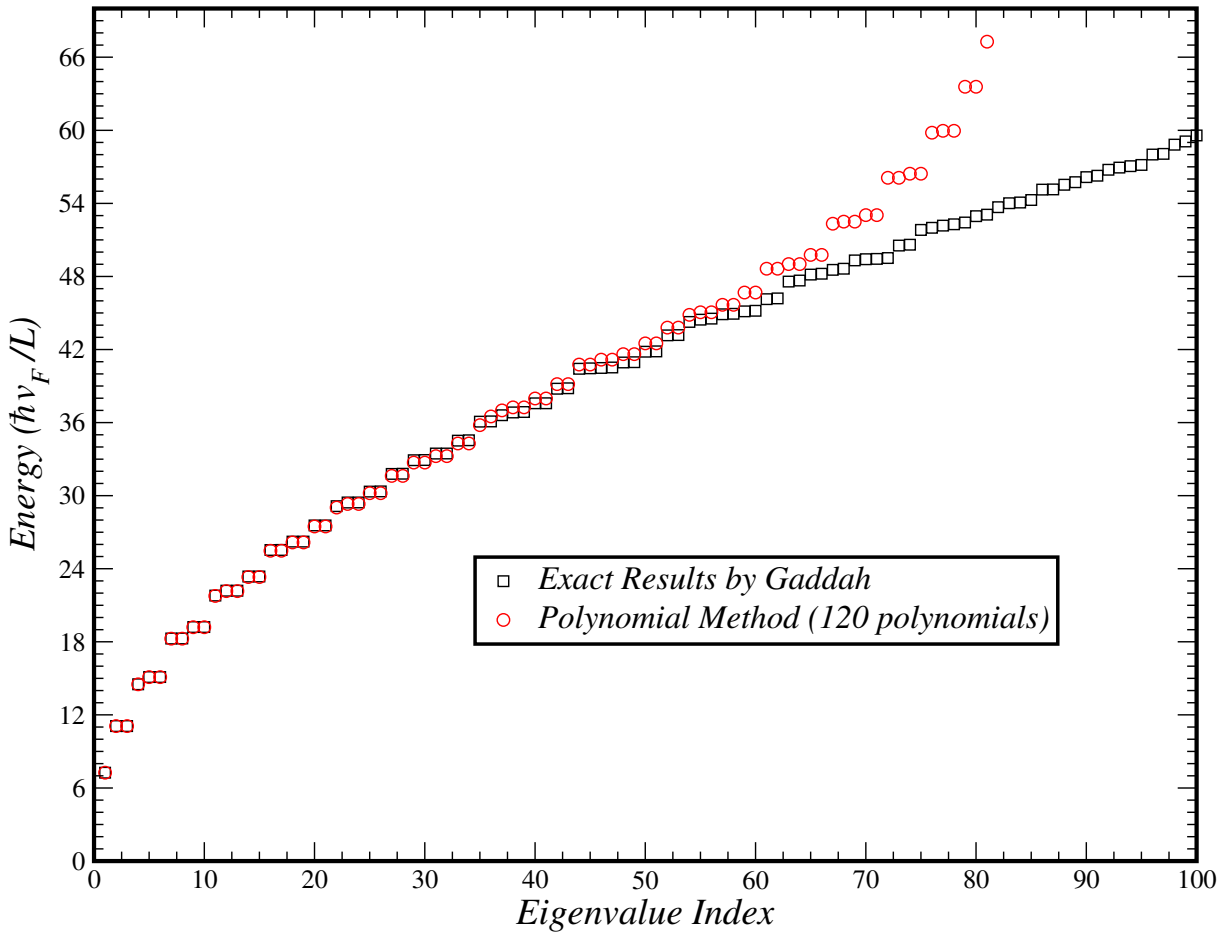

# Polynomial Method

With this, we compare $|\psi_A|^2$ for the first three eigenfunctions.

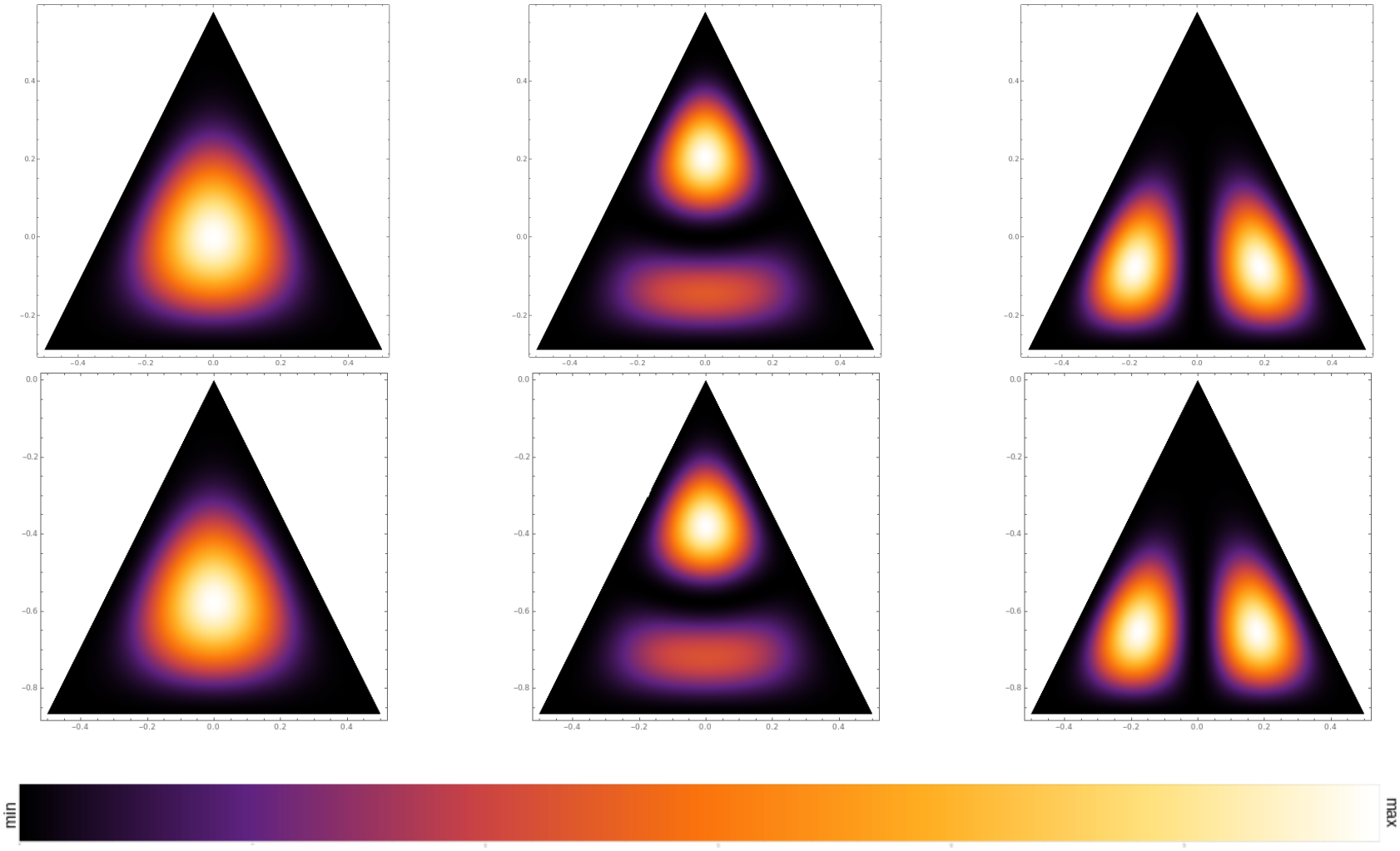

# Creating Spinors by Imposing Boundary Conditions

The necessary condition to finding confined states of Dirac equation is imposing zero normal probability current

$$\vec{j}_{\text{normal}} = v_F \Psi^\dagger \vec{\sigma}_{\text{normal}} \Psi = 0$$

of which $\psi_{A(B)} = 0$ is a very specific solution.

Imposing this, we obtain the boundary condition for an edge at an $\alpha$ angle with the $x$-axis

$$\frac{\psi_B}{\psi_A} = te^{i\alpha}, \quad t \in \mathbb{R}$$

# Creating Spinors by Imposing Boundary Conditions

The necessary condition to finding confined states of Dirac equation is imposing zero normal probability current

$$\vec{j}_{\text{normal}} = v_F \Psi^\dagger \vec{\sigma}_{\text{normal}} \Psi = 0$$

of which $\psi_{A(B)} = 0$ is a very specific solution.

Imposing this, we obtain the boundary condition for an edge at an $\alpha$ angle with the $x$-axis

$$\frac{\psi_B}{\psi_A} = te^{i\alpha}, \quad t \in \mathbb{R}$$

# 1-Dimensional Test

Setting $t = 1$ is the equivalent [Berry and Mondragan (1987)] of changing the Hamiltonian as

$$\mathcal{H}_{\mathcal{K}} \to \mathcal{H}_{\mathcal{K}} + m(\vec{r})\,\sigma_z, \qquad m(\vec{r}) = \begin{cases} 0 & \text{inside} \\ +\infty & \text{outside} \end{cases}$$

This problem is solvable exactly in 1D, where we obtain the spectrum

$$E_{n,\pm} = \pm(2n+1)\,\frac{\pi}{2L}$$

# 1-Dimensional Test

Setting $t = 1$ is the equivalent [Berry and Mondragan (1987)] of changing the Hamiltonian as

$$\mathcal{H}_{\mathcal{K}} \to \mathcal{H}_{\mathcal{K}} + m\left(\vec{r}\right)\sigma_z, \qquad m\left(\vec{r}\right) = \begin{cases} 0 & \text{inside} \\ +\infty & \text{outside} \end{cases}$$

This problem is solvable exactly in 1D, where we obtain the spectrum

$$E_{n,\pm} = \pm\left(2n+1\right)\frac{\pi}{2L}$$

# 1-Dimensional Test

A function that respects these boundary conditions in $y = \pm\frac{L}{2}$ is

$$\Psi_0(y) = N_0 \begin{bmatrix} 1 \\ -\frac{y}{L/2} \end{bmatrix}$$

The average energy of this function is

$$\langle \epsilon \rangle = -i \int_{-L/2}^{L/2} dy \Psi_0^\dagger \sigma^y \partial_y \Psi_0 = \frac{3}{2L}$$

# 1-Dimensional Test

A function that respects these boundary conditions in $y = \pm\frac{L}{2}$ is

$$\Psi_0(y) = N_0 \begin{bmatrix} 1 \\ -\frac{y}{L/2} \end{bmatrix}$$

The average energy of this function is

$$\langle \epsilon \rangle = -i \int_{-L/2}^{L/2} dy \Psi_0^\dagger \sigma^y \partial_y \Psi_0 = \frac{3}{2L}$$

# 1-Dimensional Test

The valence-band initial function for $t = 1$ will be given by

$$\Phi_0 = \sigma_x \cdot \Psi_0^*$$

When applying the G-S process, we will have to ensure both bands are orthogonal in order to define an orthonormalized basis.

# 1-Dimensional Test

The valence-band initial function for $t = 1$ will be given by

$$\Phi_0 = \sigma_x \cdot \Psi_0^*$$

When applying the G-S process, we will have to ensure both bands are orthogonal in order to define an orthonormalized basis.

# 1-Dimensional Test

Choosing a basis size, the eigenvalues of the Hamiltonian are

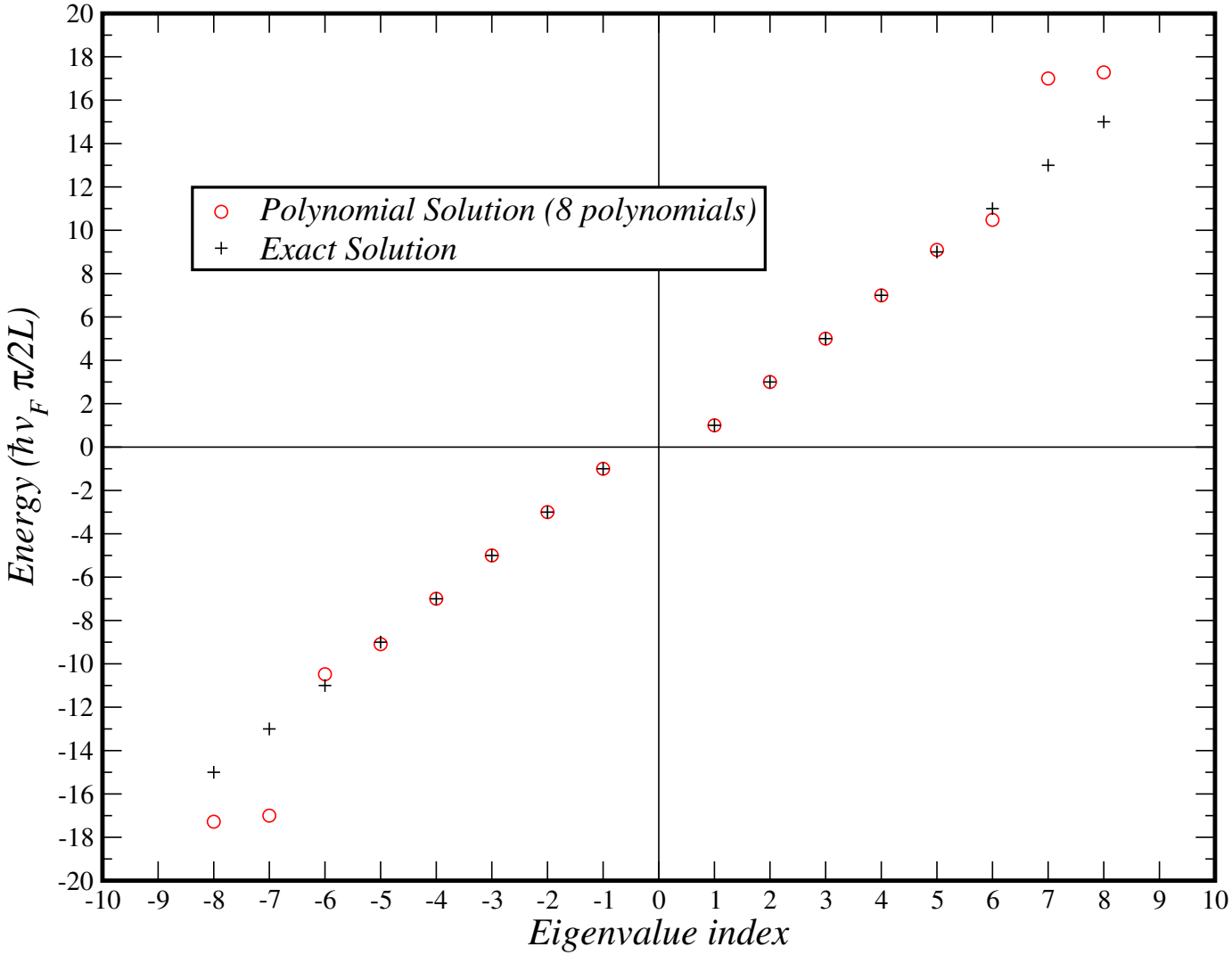

# 1-Dimensional Test

The first eigenfunction also matches perfectly:

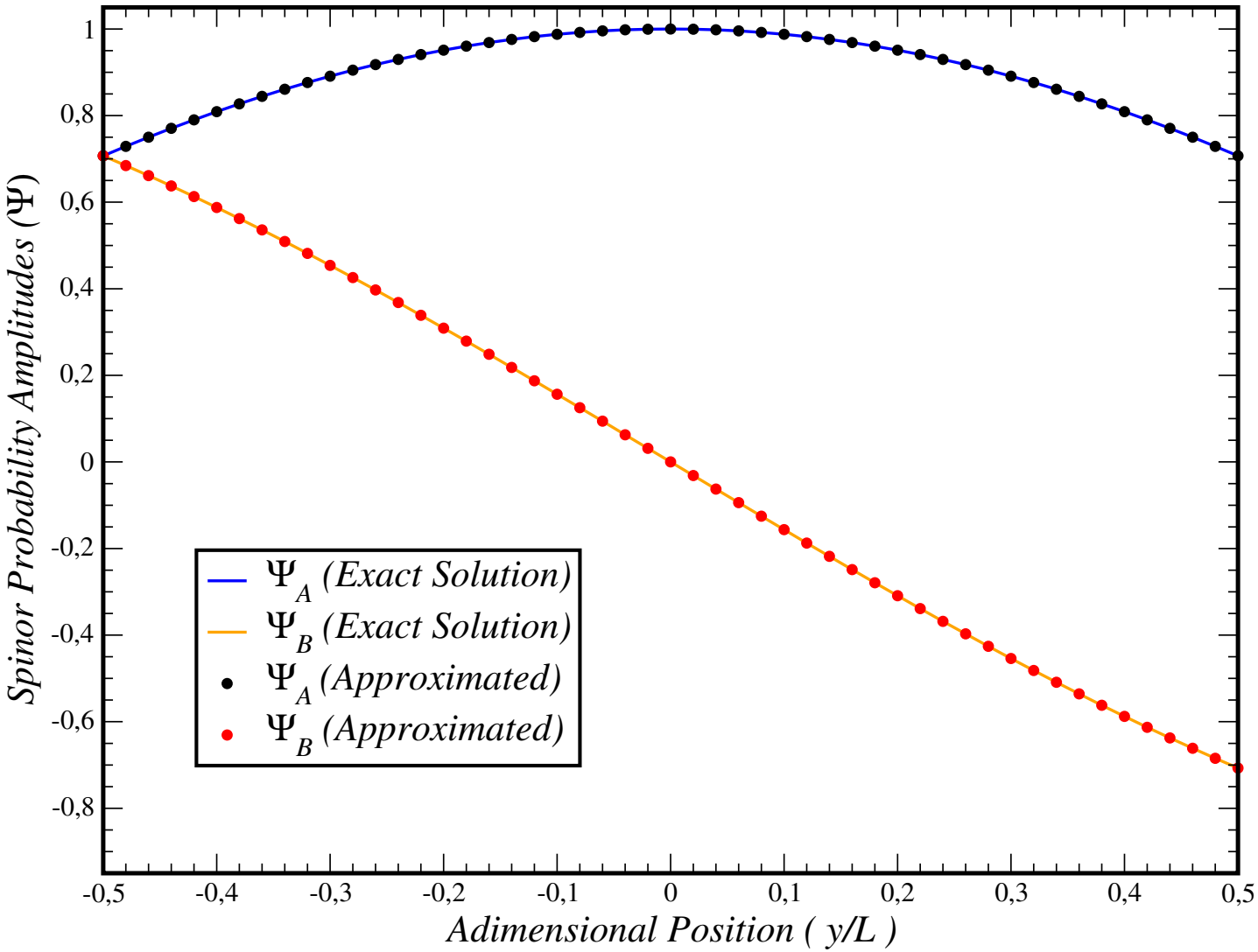

# 2-Dimensional Results: Uniform Square

To generalize this method to 2D systems, we must be careful when imposing boundary conditions.

While Dirichlet boundaries can be constructed in the same way as in the Schrödinger problem, non-Dirichlet boundaries ($t = 1$) require a more thoughtful approach.

# 2-Dimensional Results: Uniform Square

To generalize this method to 2D systems, we must be careful when imposing boundary conditions.

While Dirichlet boundaries can be constructed in the same way as in the Schrödinger problem, non-Dirichlet boundaries $(t = 1)$ require a more thoughtful approach.

# 2-Dimensional Results: Uniform Square

To preserve the ratio between the two sublattices at the boundaries, the initial spinor is constructed by adding a term for each opposing pair of edges.

$$\Psi_0(x,y) = N_0\left[\left(\frac{L^2}{4}-x^2\right)\begin{pmatrix}1\\ -\frac{2y}{L}\end{pmatrix}+\left(\frac{L^2}{4}-y^2\right)\begin{pmatrix}1\\ \frac{2ix}{L}\end{pmatrix}\right]$$

# 2-Dimensional Results: Uniform Square

To preserve the ratio between the two sublattices at the boundaries, the initial spinor is constructed by adding a term for each opposing pair of edges.

$$\Psi_0(x,y) = N_0\left[\left(\frac{L^2}{4}-x^2\right)\begin{pmatrix}1\\ -\frac{2y}{L}\end{pmatrix}+\left(\frac{L^2}{4}-y^2\right)\begin{pmatrix}1\\ \frac{2ix}{L}\end{pmatrix}\right]$$

# 2-Dimensional Results: Uniform Square

The obtained spectrum, after orthogonalization, is

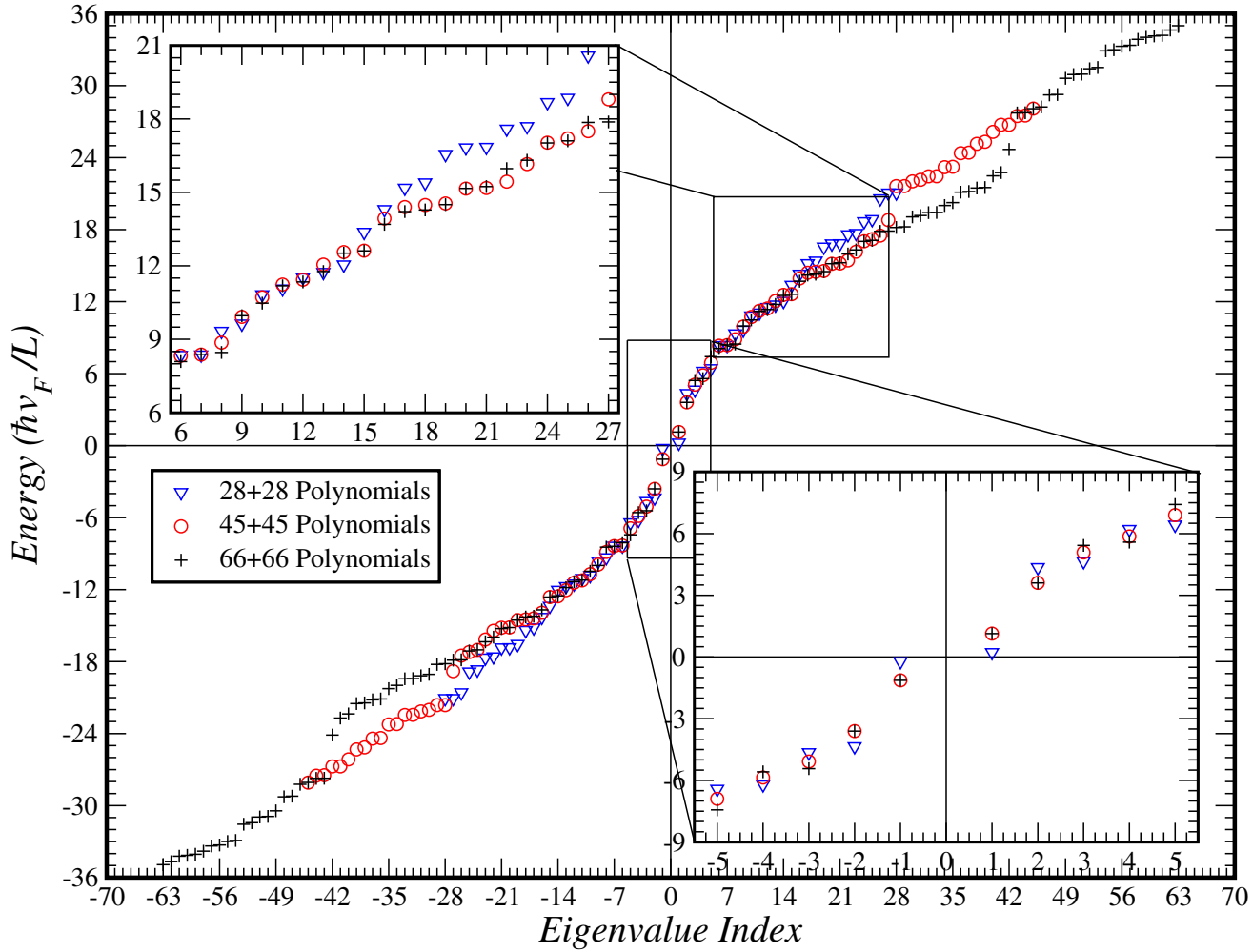

# 2-Dimensional Results: Zigzag Hexagon

In this system, the boundary conditions will switch $t \leftrightarrow t^{-1}$ when one changes edges:

- $\psi_A$-terminated, $t = \infty$;
- $\psi_B$-terminated, $t = 0$.

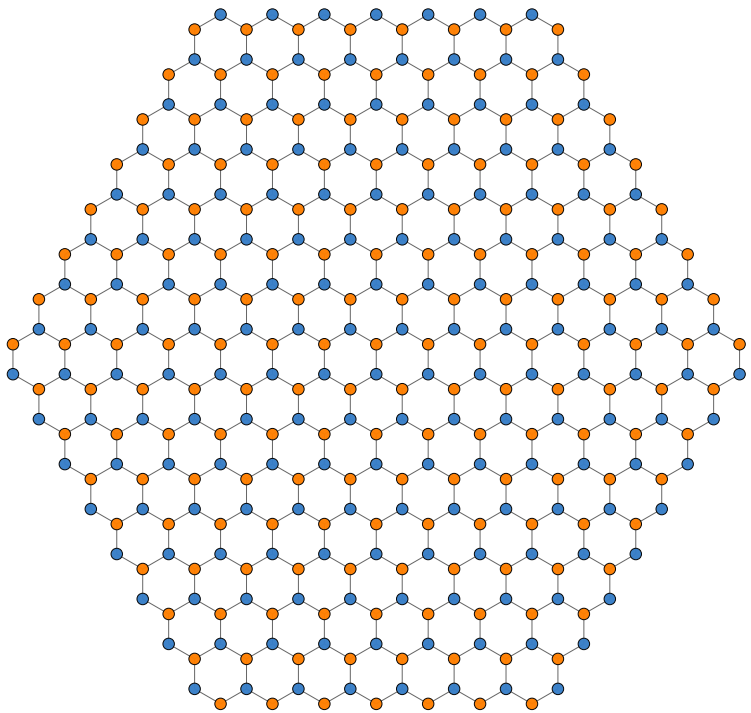

# 2-Dimensional Results: Zigzag Hexagon

As $t$ is no longer finite, adding the BCs in the extra sides will not disturb the $\psi_B/\psi_A$ ratio. As such, each spinor component will be a product of three factors of the form

$$\varphi_i(x, y) \sim y - mx - b$$

Due to the non-equivalence of the two components, the valence-band initial function will be

$$\Phi_0 = \sigma_z \cdot \Psi_0$$

# 2-Dimensional Results: Zigzag Hexagon

As $t$ is no longer finite, adding the BCs in the extra sides will not disturb the $\psi_B/\psi_A$ ratio. As such, each spinor component will be a product of three factors of the form

$$\varphi_i(x, y) \sim y - mx - b$$

Due to the non-equivalence of the two components, the valence-band initial function will be

$$\Phi_0 = \sigma_z \cdot \Psi_0$$

# 2-Dimensional Results: Zigzag Hexagon

After G-S orthogonalization, the obtained spectrum is

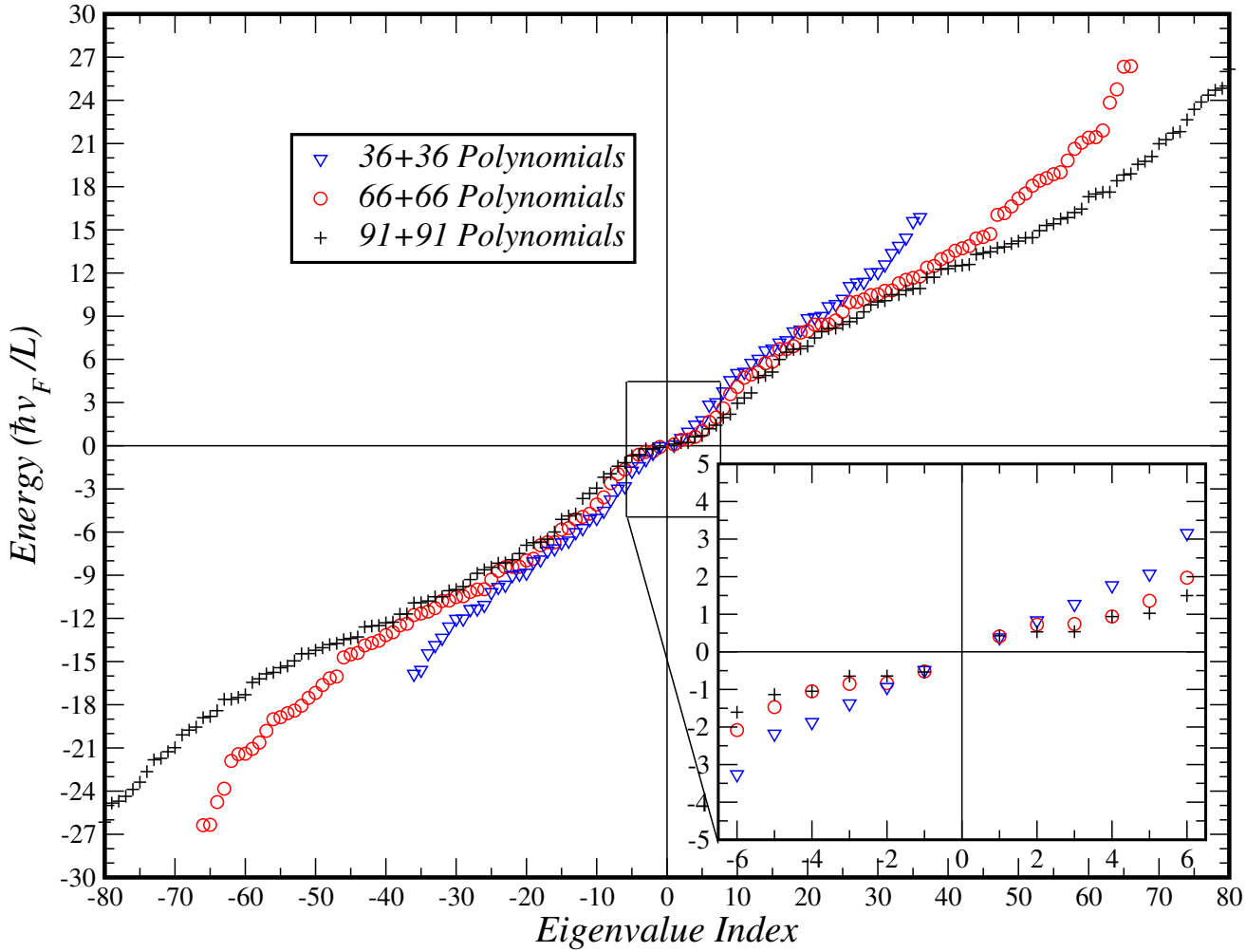

# Squaring the Hamiltonian

We can simplify this problem by squaring the Hamiltonian:

$$\begin{aligned} H^\dagger H\Psi &= -\hbar^2 v_F^2 \left(\vec{\sigma}\cdot\vec{p}\right)^\dagger \cdot \left(\vec{\sigma}\cdot\vec{p}\right)\Psi \\ &= -\hbar^2 v_F^2 \begin{pmatrix} \partial_x^2+\partial_y^2 & 0 \\ 0 & \partial_x^2+\partial_y^2 \end{pmatrix}\Psi \end{aligned}$$

This turns our problem into a one-band problem, which halves the necessary number of polynomials, significantly accelerating the calculations.

# Squaring the Hamiltonian

We can simplify this problem by squaring the Hamiltonian:

$$\begin{aligned} H^\dagger H\Psi &= -\hbar^2 v_F^2 \left(\vec{\sigma}\cdot\vec{p}\right)^\dagger \cdot \left(\vec{\sigma}\cdot\vec{p}\right)\Psi \\ &= -\hbar^2 v_F^2 \begin{pmatrix} \partial_x^2+\partial_y^2 & 0 \\ 0 & \partial_x^2+\partial_y^2 \end{pmatrix}\Psi \end{aligned}$$

This turns our problem into a one-band problem, which halves the necessary number of polynomials, significantly accelerating the calculations.

# Matrix Elements

The new matrix elements will be

$$\langle \Psi_i | H^\dagger H | \Psi_j \rangle = -\hbar^2 v_F^2 \left( \langle \psi_{i,A} | \nabla^2 | \psi_{j,A} \rangle + \langle \psi_{i,B} | \nabla^2 | \psi_{j,B} \rangle \right)$$

We calculate each of the terms in the right-hand side separately, and then study the convergence of the eigenvalues of their sum.

# Matrix Elements

The new matrix elements will be

$$\langle \Psi_i | H^\dagger H | \Psi_j \rangle = -\hbar^2 v_F^2 \left( \langle \psi_{i,A} | \nabla^2 | \psi_{j,A} \rangle + \langle \psi_{i,B} | \nabla^2 | \psi_{j,B} \rangle \right)$$

We calculate each of the terms in the right-hand side separately, and then study the convergence of the eigenvalues of their sum.

# Uniform-Boundary Square

With this method, the obtained spectrum is

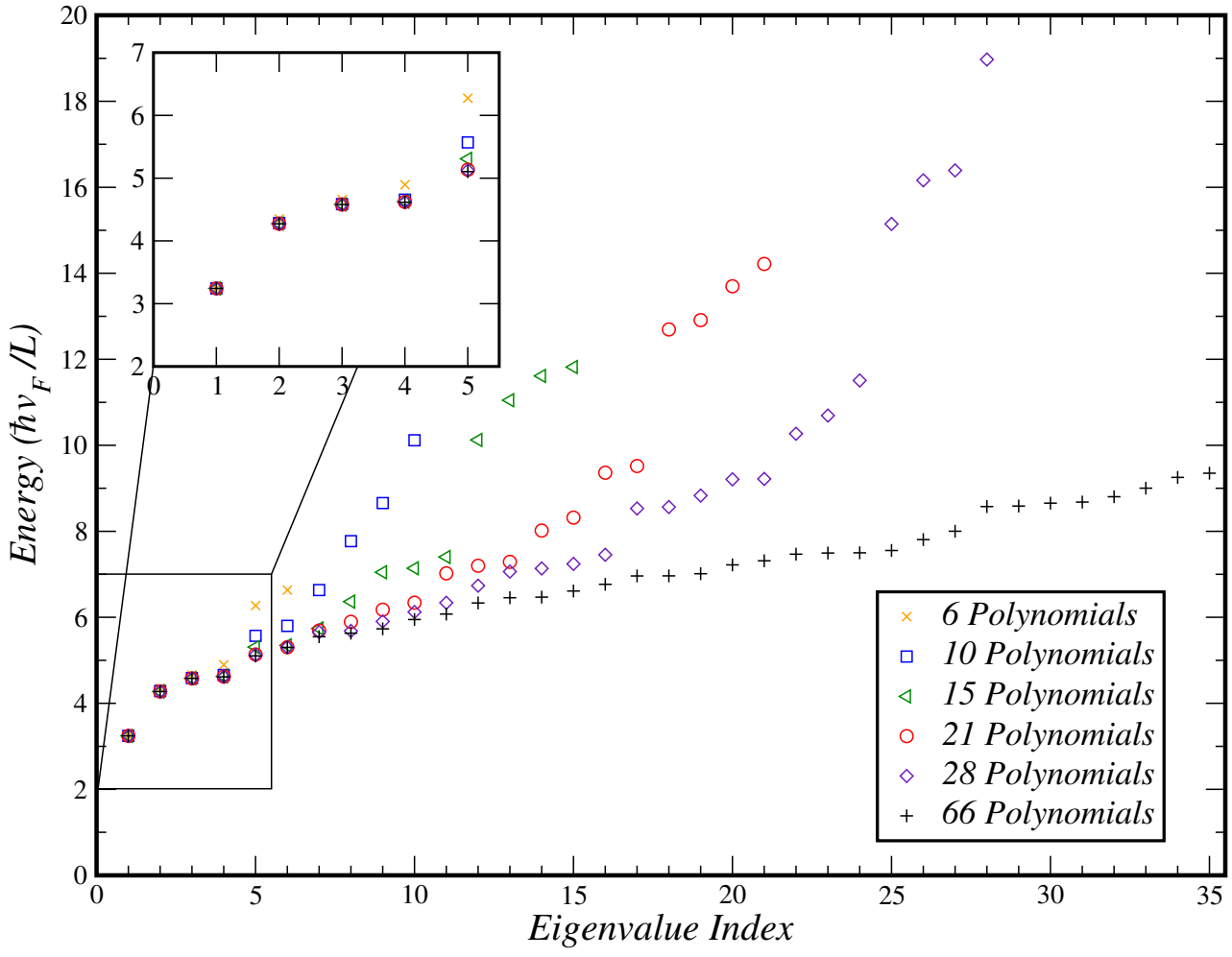

# Uniform-Boundary Square

$|\psi_A|^2 + |\psi_B|^2$ $|\psi_A|^2$ $|\psi_B|^2$

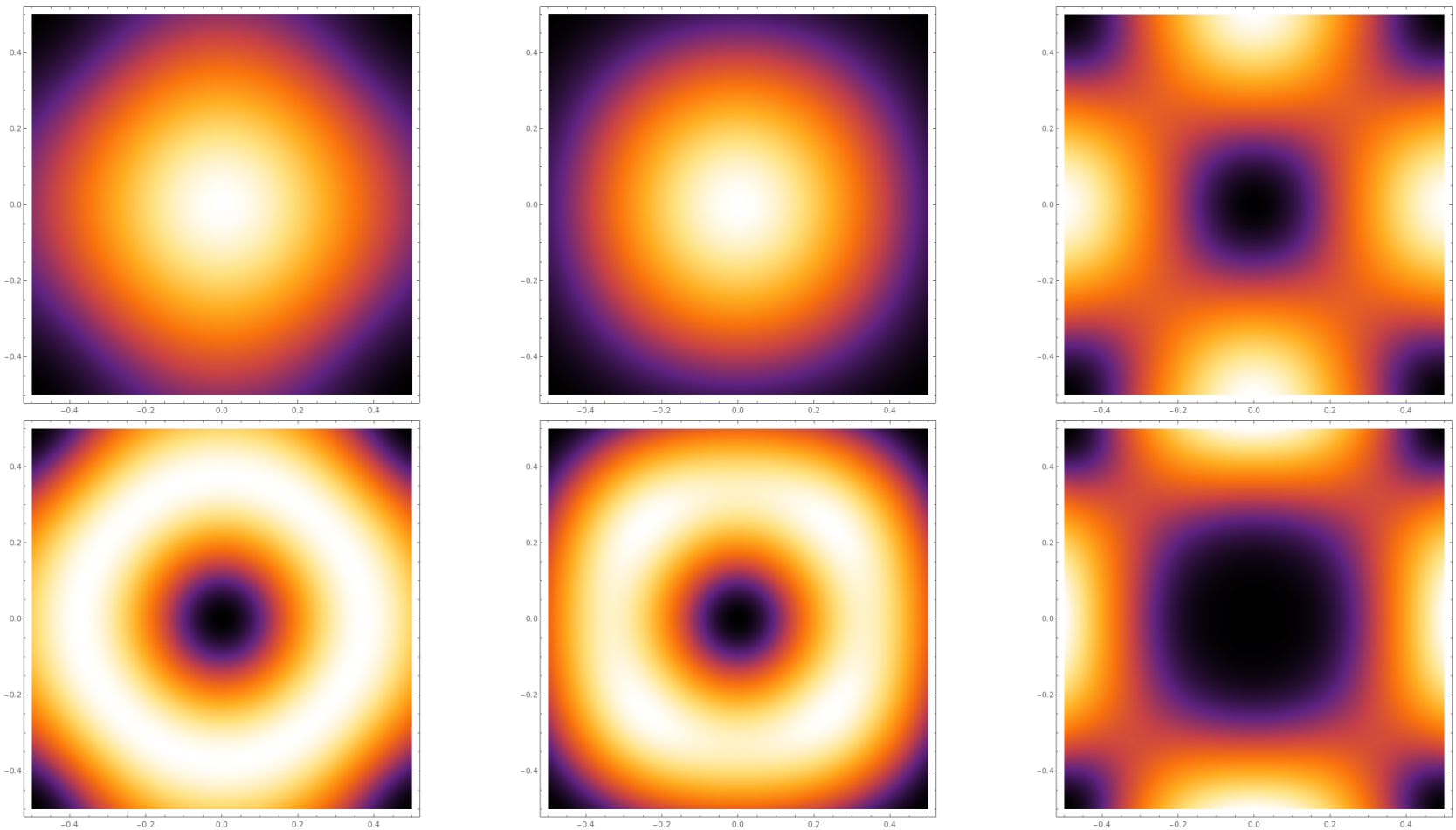


# Zigzag Hexagon

With this method, the obtained spectrum is

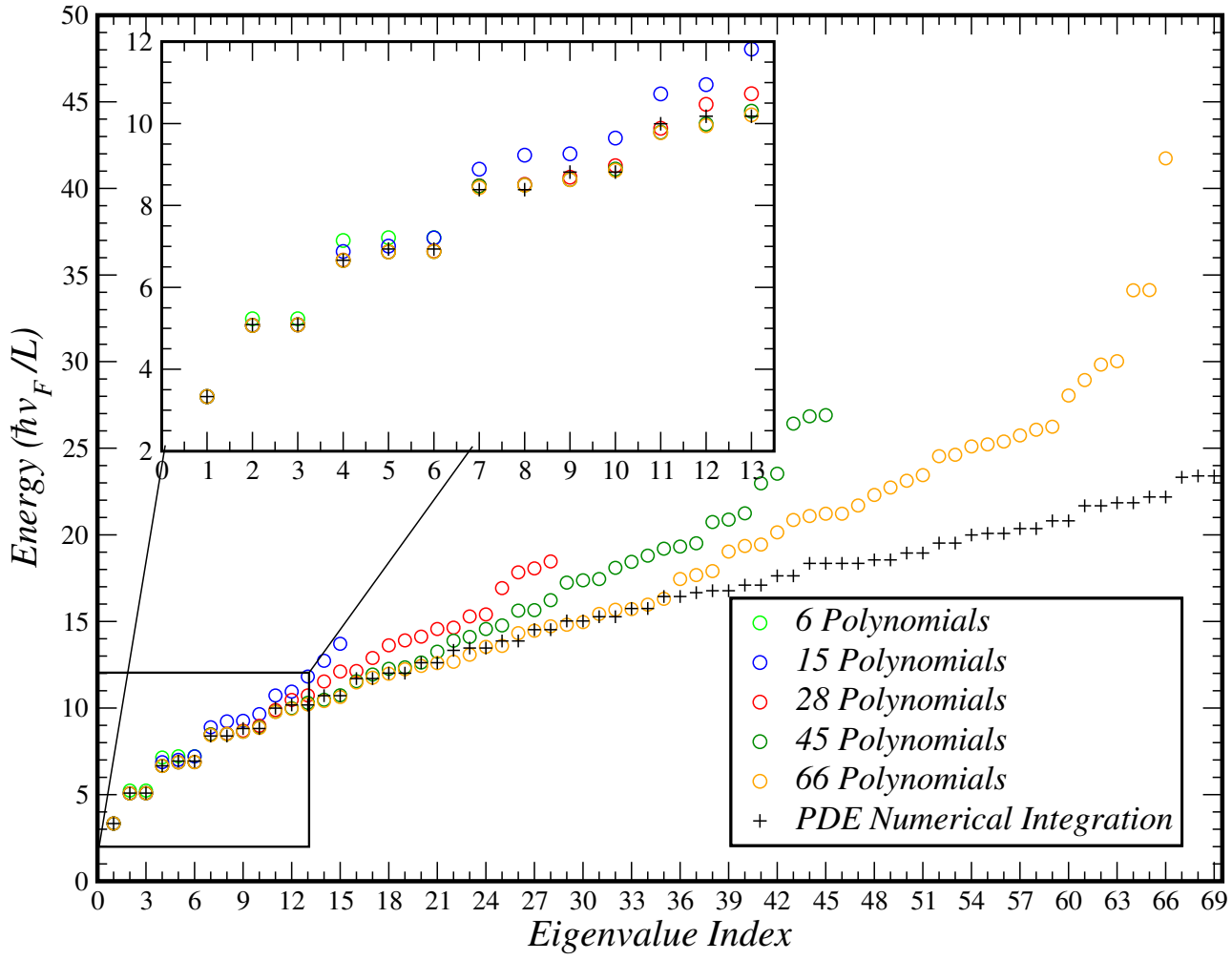

# Hexagon – Triangle Equivalence

Due to the equivalence of boundary conditions, one can imagine a symmetry between the results for the triangle and the hexagon:

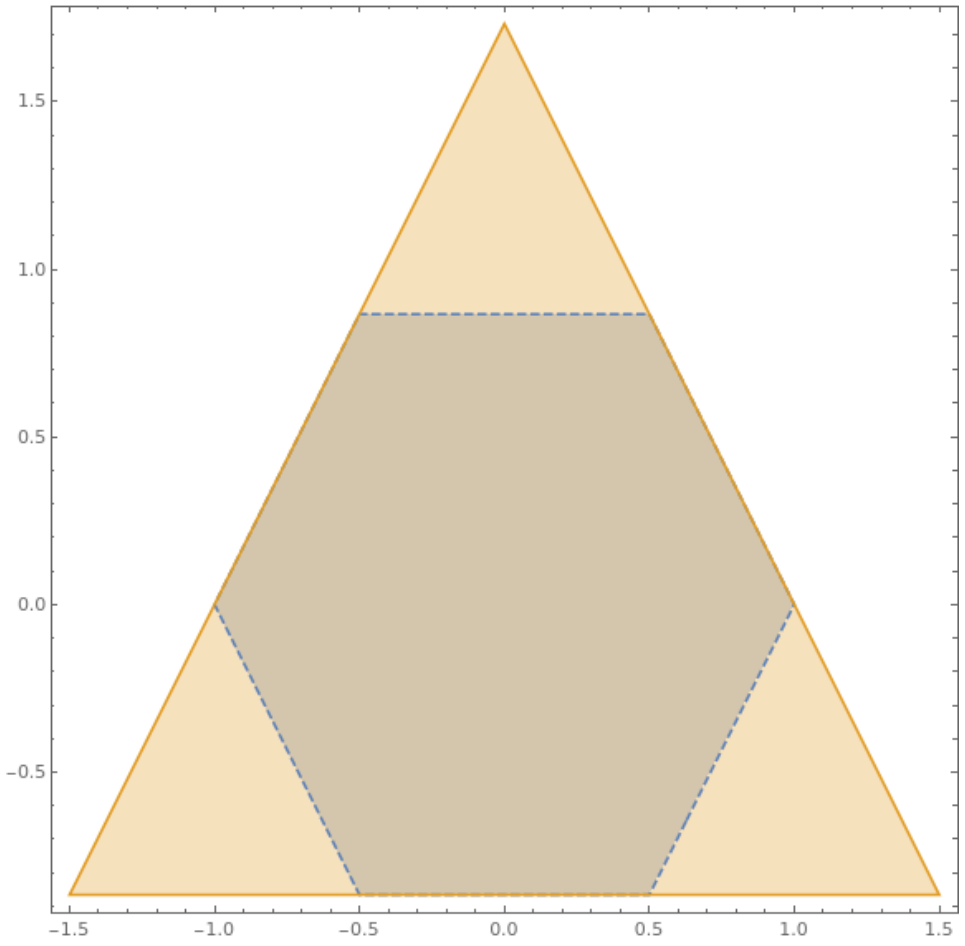

# Comparison with the Results for the Triangle

Comparing against the spectrum obtained for the zigzag triangle:

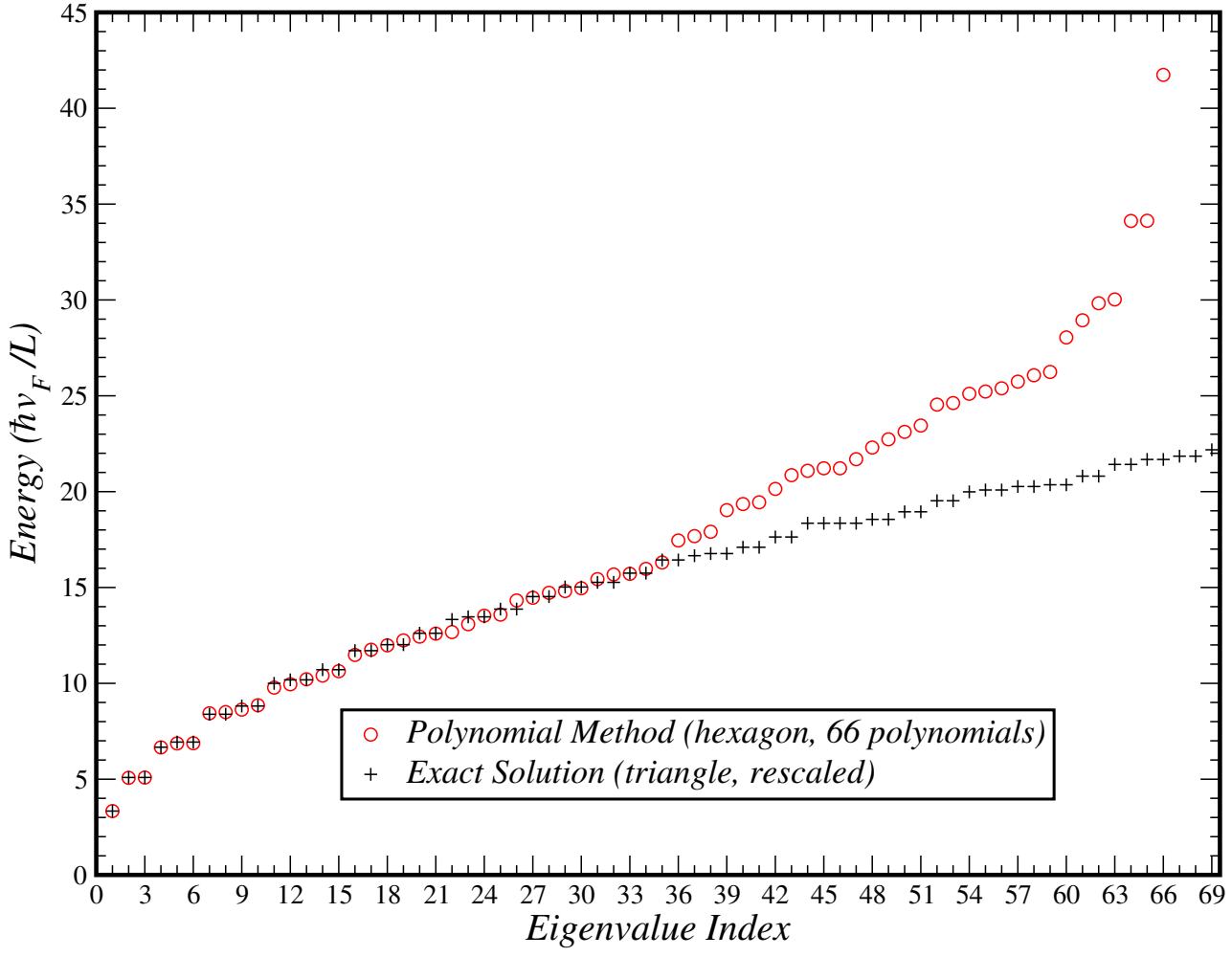

# Comparison with the Results for the Triangle

Comparing the three lowest-energy eigenfunctions for $|\psi_A|^2$:

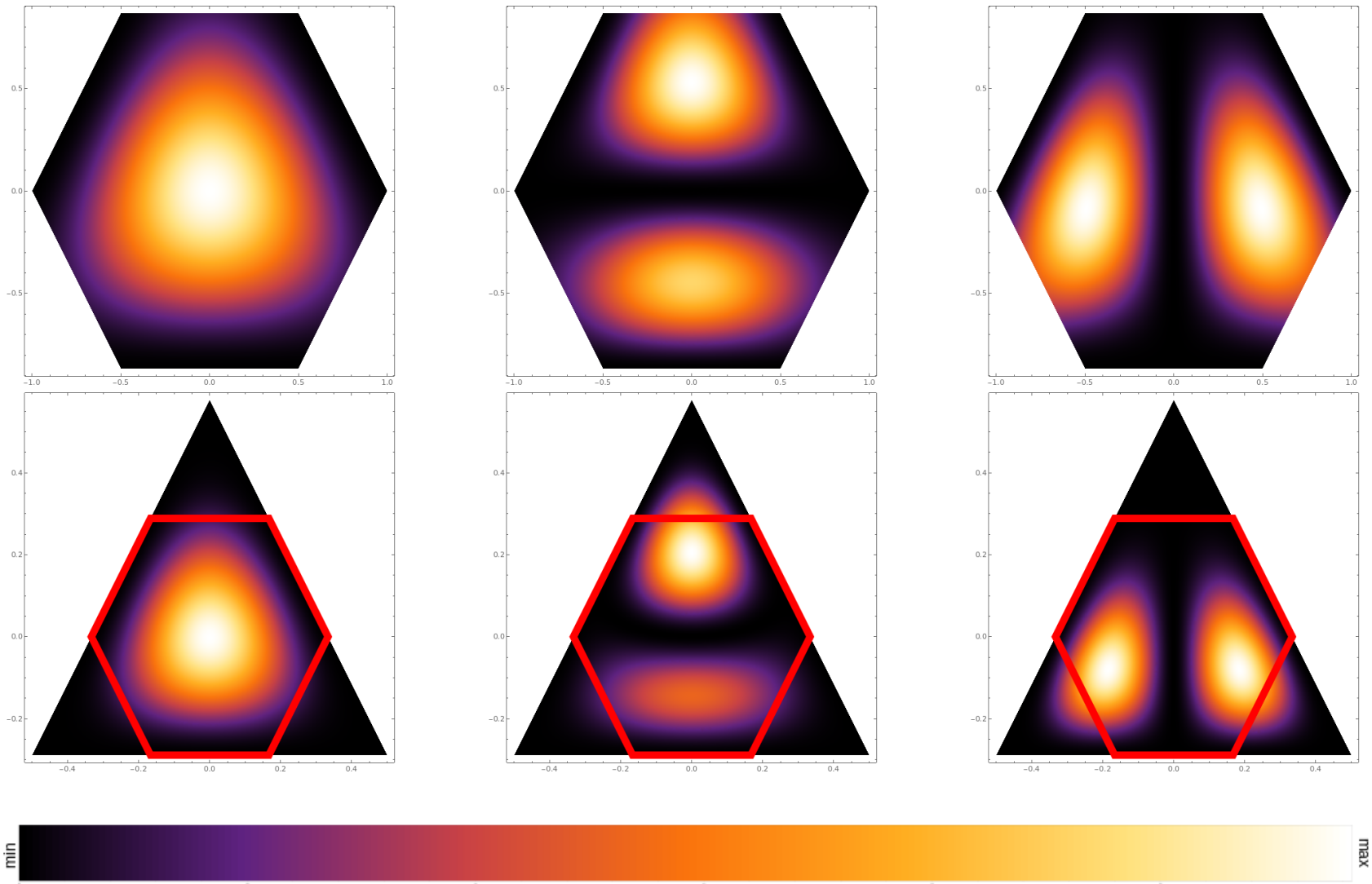

# Conclusions of this thesis

- This method allows us to replicate the exact solutions of both Dirac-Weyl and Schrödinger Equation.
- When applying directly to the Dirac-Weyl Equation, the Gram-Schmidt process has to be performed more carefully to generate the functions of both bands.

# Conclusions of this thesis

- This method allows us to replicate the exact solutions of both Dirac-Weyl and Schrödinger Equation.
- When applying directly to the Dirac-Weyl Equation, the Gram-Schmidt process has to be performed more carefully to generate the functions of both bands.

# Conclusions of this thesis

- After squaring the Dirac Hamiltonian, the calculations are significantly faster due to the existence of only one band.
- We were able to observe an apparent equivalence between the spectra of the zigzag-like triangular and hexagonal flakes.

# Conclusions of this thesis

- After squaring the Dirac Hamiltonian, the calculations are significantly faster due to the existence of only one band.
- We were able to observe an apparent equivalence between the spectra of the zigzag-like triangular and hexagonal flakes.

# Conclusions of this thesis

- Future Work?
  - The equivalence between the eigenfunctions/eigenvalues suggests the possibility of obtaining an exact solution for the hexagonal flake using the solutions for the triangular flake.
  - Applying this method to bilayer graphene seems simple enough, but the relation between the two bands and the boundary conditions has to be studied first.

# Conclusions of this thesis

- Future Work?
  - The equivalence between the eigenfunctions/eigenvalues suggests the possibility of obtaining an exact solution for the hexagonal flake using the solutions for the triangular flake.
  - Applying this method to bilayer graphene seems simple enough, but the relation between the two bands and the boundary conditions has to be studied first.

 G. Tarnopolsky, A. J. Kruchkov, and A. Vishwanath. Origin of Magic Angles in Twisted Bilayer Graphene. Physical Review Letters, 122(10):106405, March 2019.

 K. M. Liew and K. Y. Lam. A Set of Orthogonal Plate Functions for Flexural Vibration of Regular Polygonal Plates. Journal of Vibration and Acoustics, 113(2):182–186, April 1991.

 W. A. Gaddah. Exact solutions to the Dirac equation for equilateral triangular billiard systems. Journal of Physics A: Mathematical and Theoretical, 51(38):385304, September 2018.

 M. V. Berry and R. J. Mondragon Neutrino billiards: time-reversal symmetry-breaking without magnetic fields. Proceedings of the Royal Society of London. A. Mathematical and Physical Sciences, 412(1842):53–74, July 1987.

 L. Brey and H. A. Fertig. Electronic States of Graphene Nanoribbons. Physical Review B, 73(23):235411, June 2006.

 ...

The authors acknowledge financing of Fundação da Ciência e Tecnologia, of COM-PETE 2020 program in FEDER component (European Union), through projects POCI-01-0145-FEDER-028887 and UID/FIS/04650/2013. The authors also acknowledge financial support from Fundação para a Ciência e Tecnologia, Portugal, through national funds, co-financed by COMPETE-FEDER (grant M-ERA-NET2/0002/2016 – UltraGraf) under the Partnership Agreement PT2020.

Thank you!